6th International Symposium on Solid Mechanics

Click on the box to select the Mini-Symposia:

☐ Multiaxial and Fretting Fatigue (*Edgar Mamiya* and *Lucival Malcher*);

☒ Composite Materials (*Ricardo de Medeiros*);

☐ Constitutive Models I – Plasticity and Damage (*Lucival Malcher*, *Miguel Vaz Jr.* and *Edgar Mamiya*);

☐ Constitutive Models II – Viscoelastic and Viscoplastic Solids: Models and Applications (*Heraldo Mattos*);

☐ Impact Engineering (*Marcílio Alves*);

☐ Structural Reliability Methods and Reliability-Based Design Optimization (*André Beck*);

☐ Topology Optimization of Multifunctional Materials, Fluids and Structures (*Eduardo Lenz Cardoso* e *Emilio Carlos Nelli Silva*);

☐ Topological Derivatives: Theory and Applications (*André Novotny*);

☐ X-FEM, G-FEM and Meshfree Methods (*Roberto Dalledone Machado* and *Rodrigo Rossi*);

☐ High Order Finite Elements (*Marco Lúcio Bittencourt*);

☐ Nonlinear Analyses (*Eduardo Campello*);

☐ Other section;

MECSOL Joinville 2017

April 26-28, 2017

Joinville, Santa Catarina, Brazil

Application of Mori-Tanaka Method in the Evaluation of Effective Electroelastic Moduli of Porous Piezoelectric Medium

Adair Roberto Aguiar

Department of Structural Engineering

São Carlos School of Engineering, University of São Paulo, SP, Brazil

aguiarar@sc.usp.br

Julián Bravo-Castillero

Facultad de Matemática y Computación, Universidad de La Habana, Habana, Cuba

Instituto de Investigaciones en Matemáticas Aplicadas y en Sistemas,

Universidad Nacional, Autónoma de México, CDMX, Mexico

jbravo@matcom.uh.cu

Uziel Paulo da Silva

Department of Structural Engineering

São Carlos School of Engineering, University of São Paulo, SP, Brazil

uziel@sc.usp.br *

ABSTRACT

We consider a piezoelectric medium of crystal class 6mm containing a uniform distribution of empty cylindrical holes, with circular cross-sections, and use the generalized Eshelby Method together with the multiscale Mori-Tanaka Method to obtain easy-to-implement analytical formulae for the effective electroelastic properties of the medium at the macroscale. These formulae depend upon both the electroelastic properties of the matrix material and the volume fraction of the cylindrical holes. Using electromechanical properties reported in the literature, we obtain graphs of the effective properties versus the volume fraction of the pores. We then show that the effective electroelastic properties of the porous

*Corresponding author: uziel@sc.usp.br

medium decrease for increasing porous volume fraction, as expected. The results obtained via Mori-Tanaka Method agree well with results obtained via Asymptotic Homogenization Method and Finite Element Method. This work is important in the evaluation of the effective electroelastic properties of heterogeneous solids with hierarchical structures.

Keywords: Eshelby Method, Mori-Tanaka Method, Homogenization, Electroelastic Properties.

1 INTRODUCTION

In the past few decades, researchers have focused on estimating effective properties for non-homogeneous piezoelectric materials. Different schemes, such as, the Mori-Tanaka method [1, 2] and the Asymptotic Homogenization method [3] have been applied to calculate effective properties of these materials. These electroelastic materials exhibit electromechanical coupling. In fact, they can experience mechanical deformations when subjected to an electric field, and become electrically polarized under mechanical loads. The piezoelectric crystals are all dielectrics [4]. It is noticed that the symmetry of a crystal is divided into macroscopic symmetry and microscopic symmetry. There are 32 kinds of microscopic symmetry composing the 32 point-groups (crystal classes) and all crystals belong to these groups [4]. There are 11 centrosymmetric point groups with no polarization property. In the rest of the 21 groups without center of symmetry, 20 can generate the piezoelectric effect. These groups are: 1, 2, m, 222, $2mm$, 4, $\bar{4}$, 422, $4mm$, $\bar{4}2m$, 3, 32, $3m$, 6, $\bar{6}$, 622, $6mm$, $\bar{6}m2$, 23, $\bar{4}3m$. A more detailed explanation can be found in [5].

This research is motivated by the need of evaluating the effective properties of hierarchical structures and its components in several structural levels. Moreover, this work is important in the evaluation of the effective electroelastic properties of cortical bone, which can be characterized as a heterogeneous solid with a hierarchical structure. At the mesoscale, dry cortical bone can be modeled as a porous medium containing unidirectional cylindrical holes embedded in a piezoelectric matrix made of a material that belongs to the hexagonal crystal class [22]. The Eshelby tensor is a key to the determination of effective properties of piezoelectric composites. Eshelby [6] has shown that the problem of inclusions prescribed with a uniform eigenstrain embedded in an infinite elastic matrix, can be solved elegantly by using the superposition principle of linear elasticity together with the Green's function. Benveniste [2] has obtained the coupled electroelastic fields for a single ellipsoidal inclusion problem without giving estimations of averaging fields. Based upon the Green's functions derived by Deeg [17], Dunn and Taya [8] has presented estimations of the average electroelastic fields at finite concentrations and predicted the effective electroelastic moduli of a two-phase composite reinforced by ellipsoidal particles or fibers. A significant contribution to those piezoelectric problems were given by [7-9]. These authors solved the equivalent Eshelby inclusion problem for a single ellipsoidal inclusion in an infinite piezoelectric medium applying the Green's function approach. The schemes to derive the electroelastic Eshelby tensor, as well as the explicit results for the tensor components of fibrous and lamellar composites, were also given by [10-13], and, more recently, by [14, 15].

In this work, the same concept of Dunn and Taya [9] is adopted to evaluate the influence pores on the resulting electroelastic behavior. We show explicitly the Eshelby tensor for cylindrical inclusions aligned along the x_3-axis and parallel to axis of anisotropy. The components of the piezoelectric Eshelby tensor are equivalents to those obtained by [8, 17], however, we present a direct and easier way to derive the integral representation of this tensor.

In this paper, a model for piezoelectric composite is proposed. The matrix is composed by piezoelectric solid of crystal class 6mm and containing a uniform distribution of empty cylindrical holes, with circular cross sections. The generalized Eshelby tensors for the electroelastic materials are formulated analytically for ellipsoidal inclusion and together with the multiscale Mori-Tanaka Method are applied for the limit case of circular cylindrical inclusion to obtain easy-to-implement analytical formulae for the effective electroelastic properties of the medium at the macroscale. These resulting formulae depend upon both the electroelastic properties of the matrix material and the volume fraction of the cylindrical holes. By using electroelastic properties reported in [21], graphs of the effective properties versus the volume fraction of the pores are obtained. Then it is shown that the effective electroelastic properties of the porous medium decrease for increasing porous volume fraction. All numerical results of effective electroelastic moduli are in good agreement with existing results obtained via Asymptotic Homogenization Method and via Finite Element Method.

In the chapter 2 the fundamental equations for the mathematical formulation of the theory of piezoelectricity and the notation used in this work are presented. The problem is stated and the mathematical formulation to determine the Eshelby tensor is reviewed and presented in the chapter 3. In the chapter 4 the approach to the model the effective properties and the Mori-Tanaka Method are presented. Numerical results are shown in chapter 5, in which, the results are compared to the results obtained by Asymptotic Homogenization Method presented in [20] and Finite Element Method [21]. The latest chapter is a brief conclusion.

2 GOVERNING EQUATIONS FOR PIEZOELECTRICITY

In this work, the governing equations of piezoelectricity are given by

$$\begin{aligned} &\sigma_{ij,i} + f_i = 0, \\ &D_{i,i} = \rho, \end{aligned} \qquad j = 1, 2, 3, \tag{1}$$

where sum of repeated indices is implied. Also, for $i, j = 1,2,3,$ σ_{ij} are the components of the stress tensor $\boldsymbol{\sigma}$, D_i are the components of the electric displacement $\mathbf{D}$, f_i are the components of body force $\mathbf{f}$, and ρ is the free charge density. The first and second expressions in (1) are the elastic equilibrium equations and Gauss` law of electrostatic, respectively. Observe that bold face character denote matrices or vectors.

The stress tensor and the electric displacement depend linearly on the strain tensor $\boldsymbol{\varepsilon}$ and the electric field $\mathbf{E}$, i.e,

$$\begin{aligned} \sigma_{ij} &= C_{ijmn}\varepsilon_{mn} - e_{nij}E_n, \\ D_i &= e_{imn}\varepsilon_{mn} + \kappa_{in}E_n, \end{aligned} \qquad (2)$$

where, for $m,n = 1,2,3,$ the strain components ε_{mn} and electric field components E_n depend on the displacement components u_m and the electric potential φ through the relation

$$\begin{aligned} \varepsilon_{mn} &= \left(u_{m,n} + u_{n,m}\right)/2, \\ E_n &= -\varphi_{,n} \end{aligned} \qquad (3)$$

respectively. In (2), C_{ijmn}, e_{imn} and κ_{in} are the components of elastic, piezoelectric and dielectric moduli, respectively.

Next, we use the notation of Lothe and Barnet [16] to write the expressions in (1)-(3) in a compact form. For this, the lower case subscripts take on the values $1,2,3,$ and the capital subscripts take on the values $1,...,4.$ Also, repeated capital subscripts correspond to the implicit sums over the capital subscripts. Thus, the elastic strain and the electric field are expressed as the general strain-electric field defined by,

$$Z_{Mn} = \begin{cases} \varepsilon_{mn}, & M = 1,2,3, \\ -E_n, & M = 4. \end{cases} \qquad (4)$$

Similarly, we have the general displacement-electric potential

$$U_M = \begin{cases} u_m, & M = 1,2,3, \\ \varphi, & M = 4, \end{cases} \qquad (5)$$

the general stress-electric displacement

$$\Sigma_{iJ} = \begin{cases} \sigma_{ij}, & J = 1,2,3, \\ D_i, & J = 4, \end{cases} \tag{6}$$

the general body force-free charge density

$$\rho_J = \begin{cases} f_j, & J = 1,2,3, \\ -\rho, & J = 4, \end{cases} \tag{7}$$

and the electroelastic moduli

$$E_{iJMn} = \begin{cases} C_{ijmn}, & J = M = 1,2,3, \\ e_{nij}, & J = 1,2,3; M = 4, \\ e_{imn}, & J = 4; M = 1,2,3, \\ -\kappa_{in}, & J = M = 4. \end{cases} \tag{8}$$

The moduli E_{iJMn} are also called electromechanical coupling moduli.

By using the above shorthand notation, the equations (1)-(3) can be written compactly as

$$\Sigma_{iJ,i} = -\rho_J, \qquad J = 1,\ldots 4, \tag{9}$$

where

$$\Sigma_{iJ} = E_{iJMn} Z_{Mn}, \qquad i = 1,\ldots 3, J = 1,\ldots 4, \tag{10}$$

and

$$Z_{Gh} = F_{GhiJ} \Sigma_{iJ}, \qquad G = 1,\ldots,4, h = 1,\ldots,3, \tag{11}$$

where $F_{GhiJ} = E^{-1}_{iJMn}$.

Furthermore,

$$E_{iJMn} Z_{Mn} = E_{iJMn} U_{M,n}. \tag{12}$$

Substituting (12) into (10) and the resulting expression in (9), we obtain

$$E_{iJMn} U_{M,ni} = -\rho_J. \tag{13}$$

The equation (13) is the *general governing equation* for linear piezoelectric materials.

3 PROBLEM STATEMENT

In this Section, the coupled electroelastic field in an inclusion embedded in an infinite matrix is determined following the methodology proposed by [7, 8].

Consider a piezoelectric solid occupying an infinite domain, $D \subseteq \mathbb{R}^3$, and containing an inhomogeneity, Ω, of ellipsoidal shape, defined by $(x_1/a_1)^2 + (x_2/a_2)^2 + (x_3/a_3)^2 = 1$, where a_1, a_2 and a_3 are lengths of the semiaxes of the ellipsoid. The inhomogeneity can be modeled by an equivalent inclusion [6, 7, 17]. The material inside Ω is called an inclusion and the material outside Ω is called the matrix. First, consider the inclusion with the same electroelastic moduli of the matrix, E_{iJMn}. The inclusion is allowed to be under a uniform strain free of stress, ε^*_{mn}, and undergo an electric field free of electric displacement, E^*_n. Recalling the notation of section 2, we then have that the general strain-electric field of the inclusion may be represented by Z^*_{Mn}, as illustrated in Fig. 1.

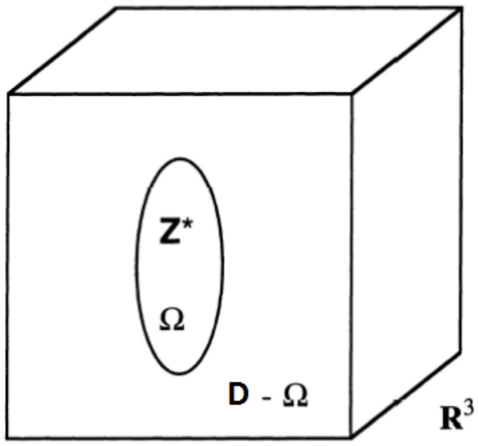

Fig. 1. $\mathbf{Z}^*$ is the eigenstrain-electric field in a region $\mathbf{\Omega}$ in an infinite piezoelectric medium $D \subseteq \mathbb{R}^3$. Adapted from [12].

Consider zero body force, $\mathbf{f} = 0$, and free charge density, $\boldsymbol{\rho} = 0$. Thus, the present problem is:

$$\Sigma_{iJ,i} = 0, \tag{14}$$

$$\Sigma_{iJ} = E_{iJMn}[Z_{Mn} - Z^*_{Mn}], \tag{15}$$

$$E_{iJMn}Z_{Mn} = E_{iJMn}U_{M,n}, \tag{16}$$

where the eigenstrain-electric field, Z^*_{Mn} , is given by

$$Z^*_{Mn}(\mathbf{x}) = \begin{cases} Z^*_{Mn} & \mathbf{x} \in \Omega, \\ 0 & \mathbf{x} \in D - \Omega. \end{cases} \tag{17}$$

Substituting (15) and (16) into (14) yields

$$E_{iJMn} U_{M,ni} = E_{iJMn} \partial_i Z^*_{Mn}(\mathbf{x}), \tag{18}$$

where ∂_i is the partial differentiation with respect to x_i and, by comparing (18) with (13), it is seen that $E_{iJMn} \partial_i Z^*_{Mn}(\mathbf{x})$ act as $-\rho_J$.

On the other side, the elastic displacement and electric potential, U_M , can be determined using the Green's functions, $G_{MJ}(\mathbf{x}-\mathbf{x}')$, as [7,17-18]:

$$U_M(\mathbf{x}) = \iint_{|\Omega|} G_{MJ}(\mathbf{x}-\mathbf{x}') \Sigma^*_{iJ} n_i dS(\mathbf{x}') - \iint_{|\Omega|}\int G_{MJ}(\mathbf{x}-\mathbf{x}') \Sigma^*_{iJ,i} dV(\mathbf{x}'), \tag{19}$$

where n_i is component normal to $|\Omega|$. By [17], the Green's function in the expression (19), may be expressed as

$$G_{MJ}(\mathbf{x}-\mathbf{x}') = \frac{1}{8\pi^2 |\mathbf{x}-\mathbf{x}'|} \int_{|\mathbf{z}|=1} K^{-1}_{MR} \delta(\mathbf{z} \cdot \mathbf{t}) dS(\mathbf{z}), \tag{20}$$

where $\delta(\mathbf{x})$ is the Dirac delta function, $|\mathbf{z}| = 1$ is the surface of the unit sphere centered at $\mathbf{z} = 0$, and K^{-1}_{MR} is the inverse of

$$K_{JR} = z_i z_n E_{iJRn} = z_i z_n E_{iRJn} \tag{21}$$

and $\mathbf{t}$ is the normalized vector $\mathbf{t} = (\mathbf{x}\text{-}\mathbf{x}')/|\mathbf{x}\text{-}\mathbf{x}'|$

Following the works of [17] and [7], by using the properties of the Dirac delta function, the derivative $U_{M,n}(\mathbf{x})$, can be expressed as

$$U_{M,n}(\mathbf{x}) = \frac{a_1 a_2 a_3}{4\pi} E_{iJAb} Z^*_{Ab} \int_{|\mathbf{z}|=1} \frac{1}{\zeta^3} z_i z_n K^{-1}_{MJ}(\mathbf{z}) d\Omega(\mathbf{z}), \tag{22}$$

where $\zeta = \left(a_1^2 z_1^2 + a_2^2 z_2^2 + a_3^2 z_3^2\right)^{\frac{1}{2}}$.

Due to the linearity, the strain-electric field, $Z_{Mn} = \left(U_{M,n} + U_{N,m}\right)/2$, can be expressed as linear function of Z_{Ab}^{*}, that is,

$$Z_{Mn} = S_{MnAb} Z_{Ab}^{*} \quad \text{in } \Omega, \tag{23}$$

where S_{MnAb} is the piezoelectric analogue to Eshelby Tensor [6], which is given by

$$S_{MnAb} = \begin{cases} \dfrac{a_1 a_2 a_3}{8\pi} E_{iJAb} \displaystyle\int_{|\mathbf{z}|=1} \dfrac{1}{\zeta^3} \left[GmJin(\mathbf{z}) + GnJim(\mathbf{z})\right] dS(\mathbf{z}), M = 1,2,3, \\ \dfrac{a_1 a_2 a_3}{4\pi} E_{iJAb} \displaystyle\int_{|\mathbf{z}|=1} \dfrac{1}{\zeta^3} \left[G4Jin(\mathbf{z})\right] dS(\mathbf{z}) \;\; M = 4, \end{cases} \tag{24}$$

where

$$G_{MJin}(\mathbf{z}) = z_i z_n K_{MJ}^{-1}(\mathbf{z}). \tag{25}$$

Eshelby's tensor is known to be the key to the study of effective properties of composite materials containing ellipsoidal inclusions.

3.1 Determination of the Generalized Eshelby Tensor

The piezoelectric Eshelby tensor is defined by [12]

$$S_{MnAb} = \begin{cases} \dfrac{1}{8\pi} E_{iJAb} \left(A_{inmJ} + A_{imnJ}\right), M = (m) = 1,2,3, \\ \dfrac{1}{4\pi} E_{iJAb} A_{in4J}, \; M = 4, \end{cases} \tag{26}$$

where

$$A_{inMJ} := a_1 a_2 a_3 \int_{|\mathbf{z}|=1} \frac{1}{\zeta^3} G_{MJin}(\mathbf{z}) dS(\mathbf{z}). \tag{27}$$

The equation (27) can be transformed as follows

$$A_{inMJ} = \int_{|\boldsymbol{\mu}|=1} G_{MJin}\left(\frac{\zeta\mu_1}{a_1}, \frac{\zeta\mu_2}{a_2}, \frac{\zeta\mu_3}{a_3}\right) dS(\boldsymbol{\mu}), \tag{28}$$

where

$$\mu_1 = \frac{a_1 z_1}{\zeta},\ \mu_2 = \frac{a_2 z_2}{\zeta},\ \mu_3 = \frac{a_3 z_3}{\zeta}, \tag{29}$$

and

$$dS(\boldsymbol{\mu}) = \left(a_1 a_2 a_3 / \zeta^3\right) dS(\mathbf{z}) \tag{30}$$

According to [12], Green's functions are homogenous functions of degree zero, that means,

$$A_{inMJ} = \int_{|\boldsymbol{\mu}|=1} G_{MJin}\left(\frac{\mu_1}{a_1}, \frac{\mu_2}{a_2}, \frac{\mu_3}{a_3}\right) dS(\boldsymbol{\mu}). \tag{31}$$

Taking

$$\begin{aligned} &\mu_1 = \sin\theta\cos\psi, 0 \le \theta \le \pi, \\ &\mu_2 = \sin\theta\sin\psi,\ 0 \le \psi \le 2\pi, \\ &\mu_3 = \cos\psi, \end{aligned} \tag{32}$$

and, $dS = \sin\theta d\theta d\psi$, then, the equation (31) can be transformed into [12, 13]

$$A_{inMJ} = \int_0^{\pi}\int_0^{2\pi} G_{MJin}\left(\frac{\mu_1}{a_1}, \frac{\mu_2}{a_2}, \frac{\mu_3}{a_3}\right) \sin\psi d\theta d\psi. \tag{33}$$

Now take

$$a_1 = \lambda,\ \frac{a_1}{a_2} = \alpha,\ \frac{a_1}{a_3} = \beta. \tag{34}$$

Thus, substituting (34) into (33), and using the fact that $G_{MJin}(\mathbf{z})$ is a homogeneous function of degree zero [12], A_{MJin} is

$$A_{inMJ} = \int_0^{\pi}\int_0^{2\pi} G_{MJin}\left(\mu_1, \alpha\mu_2, \beta\mu_3\right) \sin\psi d\theta d\psi. \tag{35}$$

For a circular cylindrical inclusion along the x_3 - axis, take $\alpha = 1$ and the limit of $\beta \to 0$. Substituting (25) into (35), the non-zero components of A_{inMJ} are only

$$\begin{aligned} A_{11MJ} &= \int_0^{\pi}\int_0^{2\pi} \mu_1^2 K_{MJ}^{-1}\left(\mu_1, \mu_2, 0\right)\sin\psi d\theta d\psi, \\ A_{22MJ} &= \int_0^{\pi}\int_0^{2\pi} \mu_2^2 K_{MJ}^{-1}\left(\mu_1, \mu_2, 0\right)\sin\psi d\theta d\psi, \quad MJ = 11, 22, 33, 34, 44, \\ A_{1212} &= \int_0^{\pi}\int_0^{2\pi} \mu_1\mu_2 K_{MJ}^{-1}\left(\mu_1, \mu_2, 0\right)\sin\psi d\theta d\psi. \end{aligned} \tag{36}$$

The above results coincide with the results by [12], except of a few typographical error, when the inclusion is a circular cylindrical inclusion.

Now, to obtain K_{MJ}^{-1}, consider the problem of the piezoelectricity of a hexagonal material belonging to the piezoelectric crystal class 6*mm* (see for instance [5]) subjected to electroelastic loadings. The constitutive equations (2) for that electroelastic field are expressed as

$$\begin{Bmatrix} \sigma_1 \\ \sigma_2 \\ \sigma_3 \\ \sigma_4 \\ \sigma_5 \\ \sigma_6 \\ D_1 \\ D_2 \\ D_3 \end{Bmatrix} = \begin{bmatrix} c_{11} & c_{12} & c_{13} & 0 & 0 & 0 & 0 & 0 & e_{31} \\ c_{12} & c_{11} & c_{13} & 0 & 0 & 0 & 0 & 0 & e_{31} \\ c_{13} & c_{13} & c_{33} & 0 & 0 & 0 & 0 & 0 & e_{33} \\ 0 & 0 & 0 & c_{44} & 0 & 0 & 0 & e_{15} & 0 \\ 0 & 0 & 0 & 0 & c_{44} & 0 & e_{15} & 0 & 0 \\ 0 & 0 & 0 & 0 & 0 & c_{66} & 0 & 0 & 0 \\ 0 & 0 & 0 & 0 & e_{15} & 0 & -k_{11} & 0 & 0 \\ 0 & 0 & 0 & e_{15} & 0 & 0 & 0 & -k_{11} & 0 \\ e_{31} & e_{31} & e_{33} & 0 & 0 & 0 & 0 & 0 & -k_{33} \end{bmatrix} \begin{Bmatrix} \varepsilon_1 \\ \varepsilon_2 \\ \varepsilon_3 \\ \varepsilon_4 \\ \varepsilon_5 \\ \varepsilon_6 \\ \Phi_{,1} \\ \Phi_{,2} \\ \Phi_{,3} \end{Bmatrix} \tag{37}$$

By using the definitions (8), (21) and the expression (37), K_{MJ} is expressed as

$$K_{MJ} = \begin{bmatrix} C_{imjn}\mu_i\mu_n & e_{imn}\mu_i\mu_n \\ e_{nij}\mu_i\mu_n & -\kappa_{in}\mu_i\mu_n \end{bmatrix}. \tag{38}$$

Calculating the contractions in (38), K_{MJ}, reduce to

$$K_{MJ} = \begin{pmatrix} c_{11}\mu_1^2 + \frac{1}{2}\left(c_{11} - c_{12}\right)\mu_2^2 & \frac{1}{2}\left(c_{11} + c_{12}\right)\mu_1\mu_2 & 0 & 0 \\ \frac{1}{2}\left(c_{11} + c_{12}\right)\mu_1\mu_2 & \frac{1}{2}\left(c_{11} - c_{12}\right)\mu_1^2 + c_{11}\mu_2^2 & 0 & 0 \\ 0 & 0 & c_{44}\left(\mu_1^2 + \mu_2^2\right) & e_{15}\left(\mu_1^2 + \mu_2^2\right) \\ 0 & 0 & e_{15}\left(\mu_1^2 + \mu_2^2\right) & -k_{11}\left(\mu_1^2 + \mu_2^2\right) \end{pmatrix}. \quad (39)$$

Upon inverting $K_{MJ}\left(\boldsymbol{\mu}\right)$ of expression (39), $K_{MJ}^{-1}\left(\boldsymbol{\mu}\right)$ can be expressed as

$$K_{MJ}^{-1} = \begin{pmatrix} K_{11}^{-1} & K_{12}^{-1} & 0 & 0 \\ K_{12}^{-1} & K_{22}^{-1} & 0 & 0 \\ 0 & 0 & K_{33}^{-1} & K_{34}^{-1} \\ 0 & 0 & K_{34}^{-1} & K_{44}^{-1} \end{pmatrix} \quad (40)$$

where

$$\begin{aligned} K_{11}^{-1} &= \frac{c_{11}\left(\mu_1^{\,2} + 2\mu_2^{\,2}\right) - c_{12}\mu_1^{\,2}}{c_{11}(c_{11} - c_{12})\left(\mu_1^{\,2} + \mu_2^{\,2}\right)^2}, \quad & K_{12}^{-1} &= -\frac{(c_{11} + c_{12})\mu_1\mu_2}{c_{11}(c_{11} - c_{12})\left(\mu_1^{\,2} + \mu_2^{\,2}\right)^2}, \\ K_{22}^{-1} &= \frac{c_{11}\left(2\mu_1^{\,2} + \mu_2^{\,2}\right) - c_{12}\mu_2^{\,2}}{c_{11}(c_{11} - c_{12})\left(\mu_1^{\,2} + \mu_2^{\,2}\right)^2}, \quad & K_{34}^{-1} &= \frac{e_{15}}{\left(e_{15}^2 + c_{44}k_{11}\right)\left(\mu_1^{\,2} + \mu_2^{\,2}\right)}, \\ K_{33}^{-1} &= \frac{k_{11}}{\left(e_{15}^2 + c_{44}k_{11}\right)\left(\mu_1^{\,2} + \mu_2^{\,2}\right)}, \quad & K_{44}^{-1} &= -\frac{c_{44}}{\left(e_{15}^2 + c_{44}k_{11}\right)\left(\mu_1^{\,2} + \mu_2^{\,2}\right)}. \end{aligned} \quad (41)$$

Upon substituting equations (41) into (36), and calculating the integrals in (26) the Eshelby`s tensor, S_{MnAb}, are explicitly obtained and expressed as

$$S_{MnAb} = \begin{pmatrix} \frac{5c_{11}+c_{12}}{8c_{11}} & \frac{3c_{12}}{8c_{11}}-\frac{1}{8} & \frac{c_{13}}{2c11} & 0 & 0 & 0 & 0 & 0 & \frac{e31}{2c11} \\ \frac{3c12}{8c11}-\frac{1}{8} & \frac{5c11+c12}{8c11} & \frac{c13}{2c11} & 0 & 0 & 0 & 0 & 0 & \frac{e31}{2c11} \\ 0 & 0 & 0 & 0 & 0 & 0 & 0 & 0 & 0 \\ 0 & 0 & 0 & \frac{1}{2} & 0 & 0 & 0 & 0 & 0 \\ 0 & 0 & 0 & 0 & \frac{1}{2} & 0 & 0 & 0 & 0 \\ 0 & 0 & 0 & 0 & 0 & 2\left(\frac{3}{8}-\frac{c12}{8c11}\right) & 0 & 0 & 0 \\ 0 & 0 & 0 & 0 & 0 & 0 & \frac{1}{2} & 0 & 0 \\ 0 & 0 & 0 & 0 & 0 & 0 & 0 & \frac{1}{2} & 0 \\ 0 & 0 & 0 & 0 & 0 & 0 & 0 & 0 & 0 \end{pmatrix} \quad (42)$$

Observe that the Eshelby tensor above coincide with that obtained by [10] and [12].

4 THE EFFECTIVE PROPERTIES

Consider that the medium is a two-phase piezoelectric composite perfectly bonded. By following the works of [8-9], consider the statistical homogeneity of the composite and the ergodic hypothesis. Therefore, the electroelastic moduli can be obtained by

$$\begin{aligned} \bar{\mathbf{\Sigma}} &= v_1\bar{\mathbf{\Sigma}}_1 + v_2\bar{\mathbf{\Sigma}}_2, \\ \bar{\mathbf{Z}} &= v_1\bar{\mathbf{Z}}_1 + v_2\bar{\mathbf{Z}}_2, \end{aligned} \quad (43)$$

where the subscript 1 and 2 denote the matrix and the inclusion, respectively, of the piezoelectric composite and $\mathbf{Z}$ and $\mathbf{\Sigma}$ are defined in (4) and (6), respectively. Furthermore, v_j are the volume fraction of each phase and the overbar denotes the volume average, i.e,

$$\bar{\mathbf{F}} = \langle \mathbf{F} \rangle = \tfrac{1}{\|\Omega\|}\int_{\Omega} \mathbf{F}\, d\Omega, \quad (44)$$

where $\|\Omega\|$ denotes the volume of Ω.

Consider that the composite is subjected to a homogeneous elastic displacement-electric potential, or, homogeneous strain-electric field, $\mathbf{Z}^0$. The calculation of the volume averaged electroelastic fields, $\bar{\mathbf{\Sigma}}$ and $\bar{\mathbf{Z}}$, are related to the effective electroelastic moduli, $\mathbf{E}$

$$\bar{\mathbf{\Sigma}} = \mathbf{E}\bar{\mathbf{Z}}. \tag{45}$$

Through the generalization of the *average strain theorem of elasticity* [19], it can be stated that the perturbation of the strain and potential fields vanish by the integration over the domain of the entire composite, thus $\bar{\mathbf{Z}}$ is obtained as [7-9]

$$\bar{\mathbf{Z}} = \mathbf{Z}^0. \tag{46}$$

By using (43) - (46) and the constitutive equations in each phase of the composite results:

$$\mathbf{E} = \mathbf{E_1} + v_2\left(\mathbf{E_2} - \mathbf{E_1}\right)\mathbf{M}, \tag{47}$$

where $\mathbf{M}$ is called *strain-potential gradient concentration matrix*, which is related with the average strain and potential in phase two by

$$\bar{\mathbf{Z}}_2 = \mathbf{M}\bar{\mathbf{Z}} = \mathbf{M}\mathbf{Z}^0. \tag{48}$$

The concentration matrix, $\mathbf{M}$, is obtained in the next section by using the Mori-Tanaka approach.

4.1 The Mori-Tanaka Method

The Mori-Tanaka method (MT) [1] is one of the micromechanical approaches for estimating the concentration matrix, $\mathbf{M}$, which, together with the piezoelectric Eshelby's tensor are a key for predicting the electroelastic moduli $\mathbf{E}$.

In this method the concentration matrix is given by [8-9]

$$\bar{\mathbf{Z}}_2 = \mathbf{M}^{dil}\bar{\mathbf{Z}}_1, \tag{49}$$

where

$$\mathbf{M}^{dil} = [\mathbf{I} + \mathbf{S}\mathbf{E}_1^{-1}\left(\mathbf{E_2} - \mathbf{E_1}\right)]^{-1} \tag{50}$$

In the expression (50), $\mathbf{I}$ is the identity matrix and $\mathbf{S}$ is the matrix representation of the Eshelby tensor defined in (24). By using the equations (43), (48) and (49), the concentration matrix can be written as

$$\mathbf{M}^{MT} = \mathbf{M}^{dil}[v_1\mathbf{I} + v_2\mathbf{M}^{dil}]^{-1}. \quad (51)$$

Then, upon substituting the equation (51) into (47) yields

$$\mathbf{E} = \mathbf{E_1} + v_2\left(\mathbf{E_2} - \mathbf{E_1}\right)\mathbf{M}^{MT}. \quad (52)$$

When the porous phase is air, the stiffness vanishes and the dielectric permittivity is approximated by that of free space [9], κ_0; thus comparing κ_0 with the permittivity of the material, κ_0 can be neglected and $\mathbf{E_2} = 0$. However, it was proved in [9] that the assumption $\mathbf{E_2} = 0$ only works for pores that are not too slender.

In the next section we apply the above results to compare numerically the accuracy of Mori-Tanaka Method with respect to the accuracies of the Asymptotic Homogenization Method and the Finite Element Method.

4.2 Numerical Results

All computations reported in this section were obtained by programming the formulae summarized in Section 4.1 with MatLab (R2015a) and Wolfram Mathematica® 11.0. In order to verify the computational code, the analytical formulae for effective properties obtained via Mori-Tanaka (MT) approach for empty circular cylindrical inclusion embedded in an infinite medium are compared with data obtained via Asymptotic Homogenization Method (A) and via Finite Element Method (N) reported by [20] and [21], respectively. The material properties used to obtain the results shown in the figures below were taken from [21]. In Table 1 the material properties of Barium titanate ($BaTiO_3$) are presented. From 50°C to 120 °C the crystal structure of a single crystal of $BaTiO_3$ belongs to the crystal class 4mm [4]. Although the electromechanical response of this single-crystal is described according to 4mm symmetry, the response of poled polycrystalline $BaTiO_3$ is described by 6mm symmetry [23].

Table 1 The material properties of $BaTiO_3$ [21]

Barium titanate (ρ =5700 kg/m^3)										
c_{11}	c_{12}	c_{13}	c_{33}	c_{44}	c_{66}	κ_{11}	κ_{33}	e_{31}	e_{33}	e_{15}
GPa	GPa	GPa	GPa	GPa	GPa	nC/(Vm)	nC/(Vm)	C/m^2	C/m^2	C/m^2
150.4	65.63	65.94	145.5	43.86	42.37	12.8	15.1	-4.32	17.4	11.4

The numerical results for electroelastic effective constants are shown below in terms of the volume fraction v_2 of the pores. In general, an excellent agreement between the results for electroelastic effective constants obtained from both analytical methods, (A) and (MT), and the numerical method (N) is observed for the whole range of the pores volume fraction. In particular, it is remarkable that the results of this work for the effective electroelastic constants c_{44} and e_{15} are indistinguishable from those derived in [20] from (A) and exhibit better concordance to the corresponding constants than those derived from (MT) in [21]. In [21] a factor of two in the shear strains was not correctly accounted for in the Eshelby tensor.

In Fig. 2 and Fig. 3 the curves for the elastic effective constants are presented. Observe from Fig. 2 that the curves for c_{33} and c_{44} obtained via (MT) are indistinguishable from the curves obtained via (A) and (N), and the curve for c_{11} obtained via (MT) is indistinguishable from the curves obtained via the (A) and (N) for small values of v_2. In Fig. 3 the curve for c_{13} obtained via (MT) is indistinguishable from the curves obtained via (A) and (N), and the curve for c_{12} obtained via (MT) is only indistinguishable from the curves obtained via (A) and (N) for small values of v_2.

Similar conclusions can be drawn from the analysis of Fig. 4, where the curves for the piezoelectric effective constants are presented. Observe from this figure that all curves for e_{33}, e_{31} and e_{15} obtained via (MT) are indistinguishable from the curves obtained via (A) and (N). Also, in Fig. 5 the curves for the dielectric effective constants are presented. Observe from this figure that the curves for κ_{33} and κ_{11} obtained via (MT) are indistinguishable from the curves obtained via the (A) and (N).

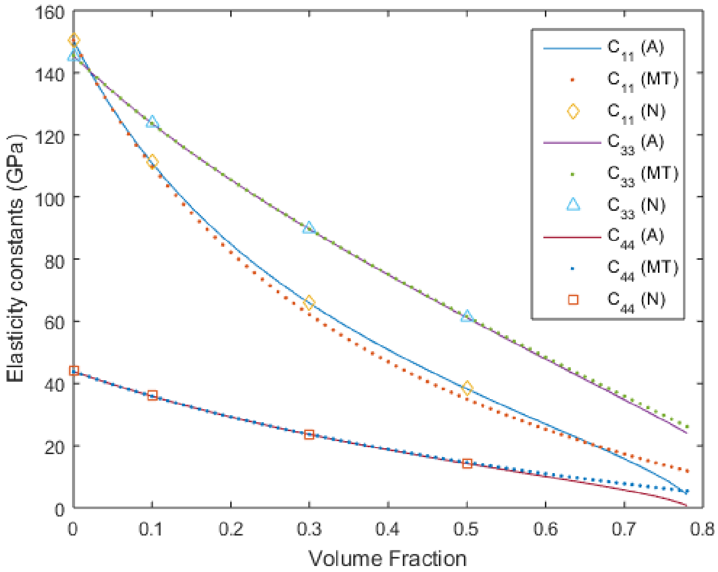

Fig. 2. Effective elastic properties for a longitudinally porous piezoelectric material. Comparison between results derived from Mori-Tanaka Method (MT) and those derived from Asymptotic Homogenization Method (A) reported by [20] and Element Method (N) reported by [21].

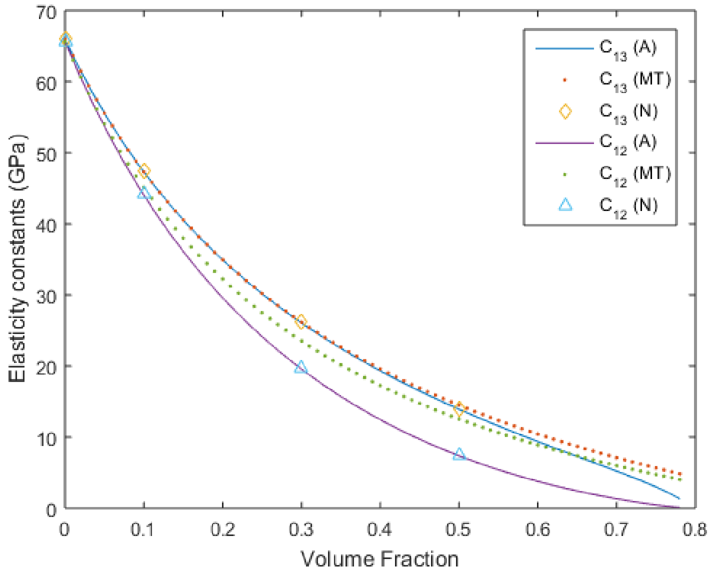

Fig. 3. Effective elastic properties for a longitudinally porous piezoelectric material. Comparison between results derived from (MT) and those derived from (A) reported by [20] and (N) reported by [21].

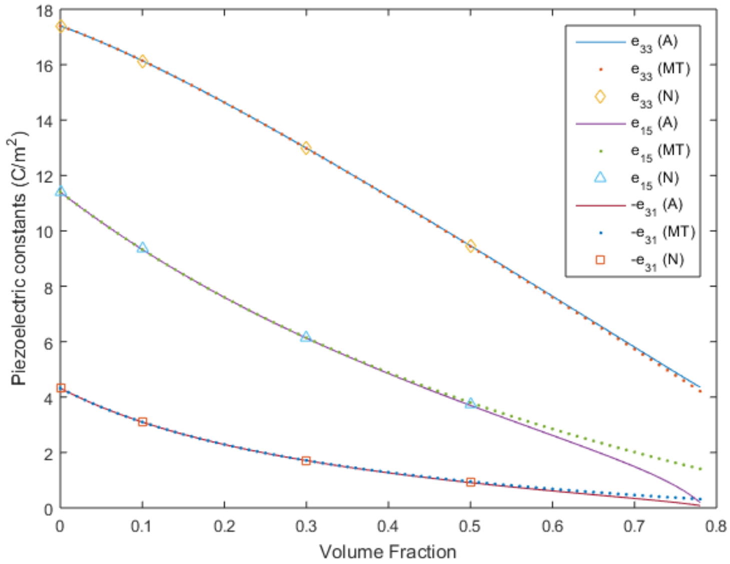

Fig. 4. Effective piezoelectric properties for a longitudinally porous piezoelectric material. Comparison between results derived from (MT) and those derived from (A) reported by [20] and (N) reported by [21].

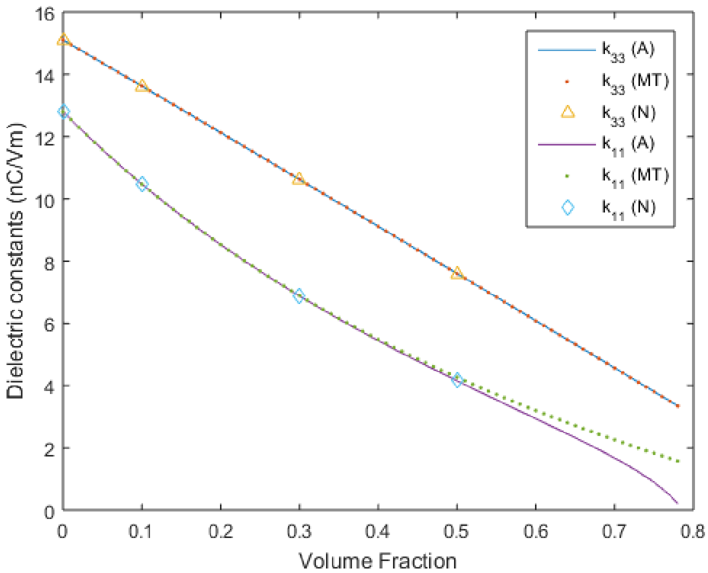

Fig. 5. Effective dielectric properties for a longitudinally porous piezoelectric material. Comparison between results derived from Mori-Tanaka Method (MT) and those derived from (A) reported by [20] and (N) reported by [21].

5 CONCLUSION

The analytical solutions for coupled electroelastic fields in a piezoelectric material of crystal class 6mm have been implemented to determine the effective properties of two-phase and porous piezoelectric solids. The Eshelby tensor was explicitly determined for circular cylindrical inclusions, which allowed the Mori-Tanaka method to yield explicit expressions for the effective electroelastic moduli. The numerical results for circular cylindrical inclusions are in good agreement with results reported in the literature, obtained from Asymptotic Homogenization Method (A) and the Finite Element Method (N).

6 ACKNOWLEDGEMENTS

The first author acknowledges the financial support from National Council for Scientific and Technological Development (CNPq), grant # 444896/2014-7, the second author is grateful to the Cátedra Extraordinaria IIMAS-UNAM, and the third author gratefully acknowledges the financial support from Coordination for the Improvement of Higher Education Personnel (CAPES) and São Paulo Research Foundation (FAPESP), grant # 2014/21836-2.

REFERENCES

[1] Mori, T. and Tanaka, K. (1973). Average Stress in Matrix and Average Elastic Energy of Materials with Misfitting Inclusions, Acta Metall., 21, 571–574.

[2] Benveniste, Y. (1987). A New Approach to the Application of Mori–Tanaka’s Theory in Composite Materials, Mech. Mater., 6, 147–157.

[3] Bravo-Castillero, J., Guinovart-Diaz, R., Sabina, F. J., and Rodrı´guez-Ramos, R. (2001). Closed-Form Expressions for the Effective Coefficients of a Fiber-Reinforced Composite with Transversely Isotropic Constituents—II. Piezoelectric and Square Symmetry, Mech. Mater., 33, 237–248.

[4] Fang, D. and Liu, J. (2013). Fracture Mechanics of Piezoelectric and Ferroelectric Solids. Tsinghua University Press, Beijing and Springer-Verlag Berlin Heidelberg.

[5] Nye, J. F. (1985). Physical properties of crystals - Their Representation by Tensors and Matrices. Clarendon Press Oxford.

[6] Eshelby, J. D. (1957). The determination of the elastic field of an ellipsoidal inclusion, and related problems, Proceedings of the Royal Society of London A: Mathematical, Physical and Engineering Sciences 241, 376–396.

[7] Dunn, M. L. and Taya, M. (1993). An analysis of piezoelectric composite materials containing ellipsoidal inhomogeneities, Proceedings of the Royal Society of London A: Mathematical, Physical and Engineering Sciences 443, 265–287.

[8] Dunn, M. L. and Taya, M. (1993). Micromechanics Predictions of the Effective Electroelastic Moduli of Piezoelectric Composites, Int. J. Solids Struct., 30, 161–175.

[9] Dunn, M. L. and Taya, M. (1993). Electromechanical Properties of Porous Piezoelectric Ceramics, J. Am. Ceram. Soc., 76, 1697–1706.

[10] Dunn, M. L. (1994). Electroelastic Green's functions for transversely isotropic piezoelectric media and their application to the solution of inclusion and inhomogeneity problems, International Journal of Engineering Science 32, 119–131.

[11] Huang, J. H. and Yu, J. S. (1994). Electroelastic Eshelby tensors for an ellipsoidal piezoelectric inclusion, Composites Engineering 4, 1169–1182.

[12] Mikata, Y. (2000). Determination of piezoelectric Eshelby tensor in transversely isotropic piezoelectric solids, International Journal of Engineering Science 38, 605–641.

[13] Mikata, Y. (2001). Explicit Determination of Piezoelectric Eshelby Tensors for a Spheroidal Inclusion. United States: N., 2001.

[14] Wang, Y., Su, Y., Li, J. and Weng, G. J. (2015). A theory of magnetoelectric coupling with interface effects and aspect-ratio dependence in piezoelectric-piezomagnetic composites, Journal of Applied Physics 117, 164106.

[15] Wang, Y. and Weng, G. J. (2016). Magnetoelectric coupling and overall properties of a class of multiferroic composites, in Advances in Nanocomposites, ed. S. A. Meguid (Springer, Switzerland), 189–233.

[16] Lothe, J. & Barnett, D.M. (1976). Integral formalism for surface waves in piezoelectric crystals. Existence considerations. J. appl. Phys. 47, 1799-1807

[17] Deeg, W.F.J. (1980). The Analysis of Dislocation, Crack, And Inclusion Problems in Piezoelectric Solids. PhD. Dissertation. Stanford University.

[18] Mura, T. (1987). Micromechanics Defects in Solids. 2 ed. Kluwer Ac. Publishers.

[19] Aboudi, J. (1991). Mechanics of composite materials. A Unified Micromechanical Approach. Elsevier, The Netherlands.

[20] Bravo-Castillero, J., Rodrıguez-Ramos, R., Guinovart-Dıaz, R., Sabina, F. J., Aguiar, A. R., Silva, U. P., and Gomez-Munoz, J. L. (2009). Analytical Formulas for Electromechanical Effective Properties of 3-1 Longitudinally Porous Piezoelectric Materials, Acta Mater., 57, 795–803.

[21] Kar-Gupta, R. and Venkatesh, T. A. (2006). Electromechanical Response of Porous Piezoelectric Materials, Acta Mater., 54, 4063–4078.

[22] Fukada, E. and Yasuda, I. (1957). On Piezoelectric Effect of Bone. J. phys. Soc. Japan, 12, 10, 1158–1162.

[23] Schwartz, R. W., et al. (2004). Piezoelectric and Electro-Optic Ceramics. In: Ceramic Materials for Electronics. 3rd ed. New York: Marcel Dekker.

RESPONSIBILITY NOTICE

The authors are the only responsible for the printed material included in this paper.